Origin of large magnetocurrent in three-terminal double-barrier magnetic tunnel junctions

S. Ladak and R. J. Hicken

Citation: J. Appl. Phys. **97**, 104512 (2005); doi: 10.1063/1.1905790
View online: http://dx.doi.org/10.1063/1.1905790
View Table of Contents: http://jap.aip.org/resource/1/JAPIAU/v97/i10
Published by the American Institute of Physics.

Origin of large magnetocurrent in three-terminal double-barrier magnetic tunnel junctions

S. Ladak and R. J. Hicken[a)]
University of Exeter, Stocker Road, Exeter, Devon EX4 4QL, United Kingdom

(Received 17 January 2005; accepted 18 March 2005; published online 11 May 2005)

Double-barrier magnetic tunnel junctions (DBMTJs) of composition $Co/AlO_x/Co/AlO_x/Ni_{81}Fe_{19}$ have been fabricated by magnetron sputtering through shadow masks. Two terminal measurements made upon the individual tunnel barriers revealed nonlinear $I-V$ curves and significant room-temperature tunnel magnetoresistance (TMR) in all cases. Measurements were also performed with connections made to all three electrodes. The TMR of a particular tunnel barrier within the DBMTJ can be strongly modified by applying a bias voltage to the other barrier, while the TMR measured across the two barriers in series decreases more slowly with increasing bias voltage than for a single barrier. With zero bias applied between the central Co base electrode and the Co collector electrode, the collector current was measured as electrons were injected from the $Ni_{81}Fe_{19}$ electrode. For structures grown on Si/SiO_2 substrates, the collector current showed a nonmonotonic dependence upon the emitter-base bias voltage, and collector magnetocurrent values in excess of 100% were observed at nonzero emitter-base bias values. For structures grown on quartz the collector current increased while the magnetocurrent decreased with increasing emitter-base voltage. We suggest that the enhanced TMR and magnetocurrent effects can be explained by substrate leakage and geometrical artifacts rather than by transport of spin-polarized hot electrons across the base layer. © *2005 American Institute of Physics*. [DOI: 10.1063/1.1905790]

I. INTRODUCTION

Magnetic tunnel junctions (MTJ's) have been the subject of much research,[1] both in fundamental studies of spin-dependent transport, and due to interest in applications in magnetic-field sensing and nonvolatile computer memory. The MTJ consists of two ferromagnetic (FM) electrodes separated by a thin insulating layer just a few nanometers thick. The resistance of the MTJ is found to depend upon the relative orientation of the electrode magnetic moments. Simple models show that the TMR depends upon the spin polarization at the Fermi level,[2] and additionally upon the spin-dependent wave vector in the case of a simple metal with a single spin-split parabolic band.[3] Tunnel magnetoresistance (TMR) values in excess of 50% have been reported for MTJs with metallic electrodes and alumina tunnel barriers.[4] However, as the bias voltage is increased, electrons are injected through the barrier with a range of excess energies and the TMR is observed to decrease.[1] While a full theoretical explanation for this decrease has yet to be developed, it is a significant disadvantage in applications where high current levels are required to achieve acceptable signal-to-noise ratio in the readout of the magnetic state.

A number of device structures have recently been reported in which the transport of spin-polarized hot electrons can be studied at energies above the Fermi level. In the spin-valve transistor[5] hot electrons pass through a metallic spin-valve structure that is confined between two Schottky barriers. In the magnetic tunnel transistor[6,7] electrons from the emitter electrode are injected through a tunnel barrier into the base electrode. Those that retain sufficient energy after crossing the base may cross a Schottky barrier into the semiconductor collector electrode. Large room-temperature collector magnetocurrent effects ($>100\%$) have been reported that result from a pronounced spin asymmetry in the Co density of states at energies of about 1 eV above the Fermi level.[8] Potential disadvantages of these devices include the rather small collector/emitter current transfer ratio, the need for epitaxial semiconductor substrates, and the difficulty of continuously tuning the height of the Schottky barrier.

Double-barrier magnetic tunnel junctions (DBMTJ's) have recently been the subject of an increasing number of theoretical and experimental studies. Two-terminal measurements performed between the outer electrodes have shown that the TMR decreases more slowly with applied bias than in an equivalent single-barrier MTJ because the voltage drop across each of the two barriers is reduced.[9] The observation of a still slower decrease in TMR with bias has been attributed to coherent transport processes.[10] Another study revealed an enhanced TMR effect at low temperature[11] that has been interpreted in terms of a "double Julliere" model that assumes coherent transport through the DBMTJ structure. However, Han *et al.*[12] instead found the TMR across a DBMTJ structure to be much smaller than predicted by the double Julliere model. The discrepancy between theory and experiment was explained in terms of the formation of current-induced vortex domains within the central electrode, which lowered the effective polarization.

DBMTJs in which a contact is made to the central electrode, have been proposed as an alternative structure in which hot-electron transport can be exploited.[13] DBMTJs provide greater flexibility in the choice of substrate, they can

[a)]Electronic mail: r.j.hicken@exeter.ac.uk

provide diode like $I-V$ characteristics[13] that may be suited to matrix addressing of logic arrays, and they allow additional flexibility in the range of excess energies that can be utilized. Although nonmagnetic three-terminal double-tunnel junctions have been studied extensively in the past,[14] only a few attempts have been made to fabricate three-terminal DBMTJs.[15,16] In each case photolithography was used to fabricate devices from a sheet material containing two tunnel barriers, although it was noted that etching may result in a damage to the tunnel barriers.[16] In one study[15] the injection of current through the first tunnel barrier was found to affect the TMR measured across the second tunnel barrier at room temperature. The results were discussed in terms of spin diffusion across the base layer. Lacour *et al.*[16] obtained evidence for the ballistic transport of hot electrons across the base layer, yet no collector magnetocurrent was observed and TMR from individual barriers was recorded only at low temperature. In the present study, we show that three-terminal DBMTJ's may be fabricated by magnetron sputtering through shadow masks. The individual tunnel barriers exhibit nonlinear $I-V$ characteristics and significant room-temperature TMR, and substantial collector magnetocurrent currents are observed. We argue that the magnetocurrent in these structures is dominated by substrate leakage effects and a geometrical artifact rather than by hot-electron transport.

II. EXPERIMENT

DBMTJs of composition substrate/Co(200 Å)/AlO_x/Co(70 Å)/AlO_x/$Ni_{81}Fe_{19}$(200 Å) were fabricated by dc magnetron sputtering through shadow masks[17] in a system with base pressure better than 4×10^{-7} Torr. Sputtering was performed at an Ar pressure of 5 mTorr while quartz-crystal oscillators were used to monitor the deposition rate. The substrate was chosen to be either thermally oxidized Si(100)/SiO_2(1000 Å) or quartz. The masks were held in a carousel driven by a vacuum-compatible stepper motor so that the entire structure could be deposited without breaking vacuum. Tunnel barriers were formed by exposing a 20-Å Al layer to a dc glow discharge in a 100 mTorr oxygen atmosphere for 5 min. In Fig. 1(a) the mask set has been superposed to show the geometry of the deposited structure which contains two separate DBMTJs. The tunnel barriers were deposited through a large area mask that covered most of the substrate. The width of the Co base (b) layer mask (1 mm) was made wider than that of the $Ni_{81}Fe_{19}$ emitter (e) and Co collector (c) masks to ensure that electrons injected from the emitter pass through the base before entering the collector. The emitter and collector masks consisted of circular junction areas of 0.5 mm diameter that were connected to bond pads by tracks with width of about 0.1 mm. The stepper motor allowed the circular regions to be aligned with sufficient accuracy that an areal overlap of about 66% (junction A) and 75.0% (junction B) was achieved between the emitter-base and base-collector junctions. The accuracy of mask alignment places a lower limit on the junction areas that can be studied. The area of a junction was approximately 20 times greater than that of the single-barrier MTJs fabricated previously in the same deposition system.[17] Thicker

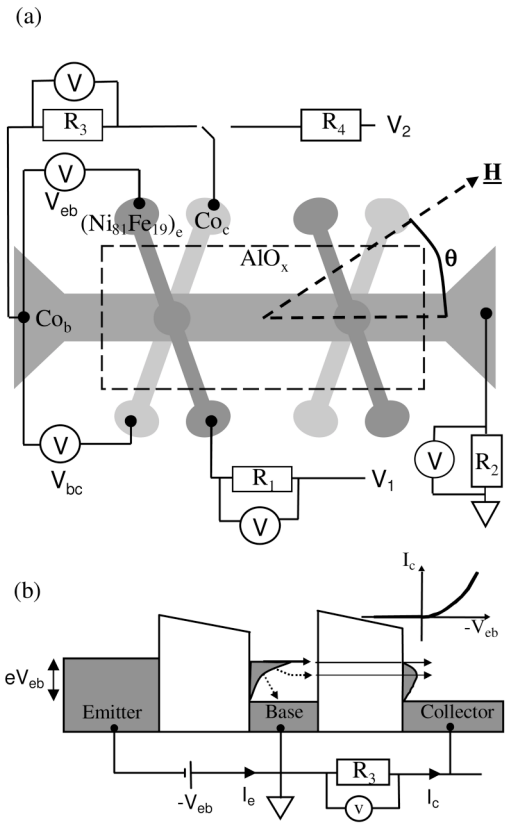

FIG. 1. (a) The mask geometry used for the double-barrier magnetic tunnel junctions is shown. The dashed rectangle indicates the area of the AlO_x tunnel barrier mask. The switch allows the selection of the three-terminal measurement configuration (b) The measurement configuration used to detect hot-electron transport is shown. The inset shows the expected form of the I_c-V_{eb} characteristic.

tunnel barriers are therefore required within the DBMTJ so that the resistance of an individual barrier remains significantly larger than the sheet resistance of the electrodes, so that current crowding effects identified in single-barrier MTJs may be avoided.[18–20]

Characterization of the samples was carried out with a spring-loaded ten-pin probe which made contact to the sample bond pads. A rotating electromagnet allowed fields of up to 5 kOe to be applied within the plane of the sample at an angle θ relative to the base electrode [see Fig. 1(a)]. A standard four-point probe technique was used to perform dc measurements upon individual tunnel barriers. $I-V$ characteristics were acquired over a ±0.5 V bias range by measuring the junction voltage and the voltage drop across a series precision resistor. The TMR measurements were carried out by applying a 20 mV bias to the junction and sweeping the magnetic field between ±1.2 kOe. Two-point probe anisotropic magnetoresistance (AMR) measurements were performed on each electrode at a fixed bias of 100–200 mV. Since the electrode resistance was in the range of 100–500 Ω in each case, the contact resistance could be neglected.

After the integrity of the individual tunnel barriers was confirmed, two types of three-terminal measurements were carried out, as shown in Fig. 1(a). The two configurations are distinguished by the presence of a switch in Fig. 1(a). In the

first, a bias voltage was applied separately to each tunnel barrier. In the second, designed to detect propagation of hot electrons across the base layer, the collector electrode was connected to the base via a resistor with a value of about one-tenth the base-collector junction resistance, as shown schematically in Fig. 1(b), and a negative bias was applied to the $Ni_{81}Fe_{19}$ emitter electrode in order to inject hot electrons into the Co base. The injected electrons are subject to spin-dependent inelastic scattering. Those that retain most energy after traversing the base are most likely to tunnel into the collector, after which they generate a small voltage drop across the series resistor as they return to the base. The I_c-V_{eb} characteristic is expected to have an infinite asymmetry with respect to positive and negative bias, with no current flowing for negative V_{eb}, as shown within the inset of Fig. 1(b). I_c-V_{eb} characteristics were acquired by sweeping the voltage V_1 applied between the emitter and base electrodes and measuring both the voltage dropped across R_3, and the voltage V_{eb} dropped across the emitter-base junction through the opposite ends of the emitter and base that take negligible current. Magnetocurrent measurements were performed by applying a fixed bias to the $Ni_{81}Fe_{19}$ emitter electrode and measuring the current in R_3 while sweeping the applied magnetic field.

III. RESULTS

More than 100 DBMTJ's were fabricated upon the quartz substrates and results are presented from just two representative samples. Some additional results will be presented for a DBMTJ fabricated on Si/SiO_2 in order to illustrate the influence of the substrate. The $I-V$ and TMR characteristics of the individual $(Ni_{81}Fe_{19})_e-Co_b$ and Co_b-Co_c junctions were first measured to confirm the integrity of the tunnel barriers. Junction resistances of 1.4 ± 0.4 kΩ for the Co_b-Co_c barrier and 0.6 ± 0.2 kΩ for the $Co_b-(Ni_{81}Fe_{19})_e$, corresponding to a resistance area product of approximately 100 MΩ μm^2, were obtained for the DBMTJs grown on quartz. We consider first a sample for which fits of the Co_b-Co_c junction $I-V$ characteristic to the Simmons model[21] corrected by Hartman[22] yielded values of $d=15.8\pm0.1$ Å for the barrier thickness and $\phi=1.94\pm0.30$ eV for the average barrier height. Values of $d=16.2\pm0.1$ Å and $\phi=1.80\pm0.30$ eV were obtained for the $Co_b-(Ni_{81}Fe_{19})_c$ junction. The thickness of the Al layer is expected to increase by a factor about 26% after oxidation.[23] However, the transport measurement probes the minimum barrier thickness which is smaller than the average physical barrier thickness due to the presence of uncorrelated interface roughness.[24]

No attempt was made to control the magnetic anisotropy of the electrodes during the sample growth. The AMR measurements revealed that all three electrodes possessed uniaxial magnetic anisotropy. The orientation of the easy axis was found to be different in each electrode, yet reproducible within the samples grown on a particular type of substrate. Figure 2 shows the TMR characteristics obtained from the individual tunnel barriers of a DBMTJ grown on quartz with the third electrode floating. The emitter, base, and collector easy axes were found to lie at $\theta=-20°$, 10°, and 20°, respectively. The orientation of the magnetic field θ was varied until the maximum TMR was observed. Maximum TMR values of approximately 10% (at $\theta=10°$) and 8% at ($\theta=30°$) were obtained for the $(Ni_{81}Fe_{19})_e-Co_b$ and Co_b-Co_c junctions, respectively. These values are somewhat smaller than those achieved previously in junctions of smaller area with thinner tunnel barriers.[17] However, the orientations yielding maximum TMR are seen to lie close to the easy axis orientations within the Co electrodes.

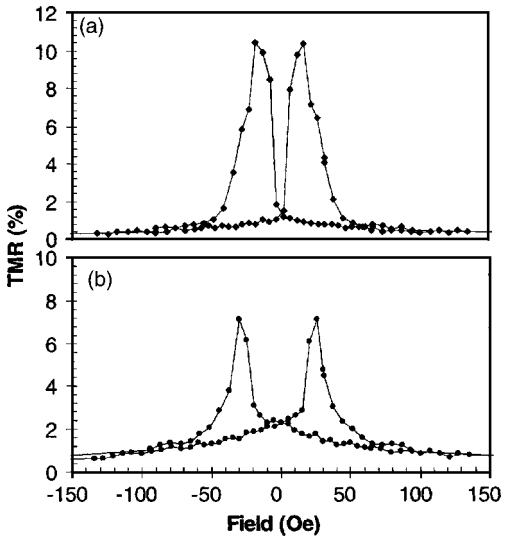

FIG. 2. TMR characteristics are shown for the individual junctions of a DBMTJ grown on a quartz substrate. The azimuths yielding the largest TMR are shown, corresponding to (a) $\theta=20°$ and (b) $\theta=50°$ for the $(Ni_{81}Fe_{19})_e-Co_b$ and Co_b-Co_c functions, respectively.

Four-point probe TMR measurements were also performed between the emitter and the collector electrodes while the base electrode was left floating. A maximum TMR of 8% was obtained with the field applied at $\theta=50°$, as shown in Fig. 3(a). The switching of each of the three electrodes can be clearly seen. Figure 3(b) shows the bias dependence of the $(Ni_{81}Fe_{19})_e-Co_b$ junction and the double-barrier TMR plotted together. The single-barrier TMR decreases to half its maximum at 310 mV whereas the double-barrier TMR falls off more slowly and reaches its half maximum at 630 mV.

TMR measurements were also performed upon the Co_b-Co_c junction as electrons were injected into the Co base from the $Ni_{81}Fe_{19}$ emitter. The applied voltage V_2 was fixed at 20 mV as V_1 was varied. Figure 4(a) shows the dependence of the measured Co_b-Co_c junction TMR and V_{bc} as a function of the measured V_{eb}. The TMR increases and reaches a maximum value at $V_{eb}=-75$ mV after which it decreases monotonically. The maximum Co_b-Co_c TMR is observed close to the point where V_{bc} changes sign. The shape of the Co_b-Co_c TMR is shown in Fig. 4(b) for different values of V_{eb}. The shape of the TMR characteristic is similar to that of the Co_b-Co_c junction shown in Fig. 2(b) for small V_{eb} but becomes increasingly similar to that of the $(Ni_{81}Fe_{19})_e-Co_b$ TMR characteristic shown in Fig. 2(a) as V_{eb} is increased.

I_c-V_{eb} and magnetocurrent measurements were per-

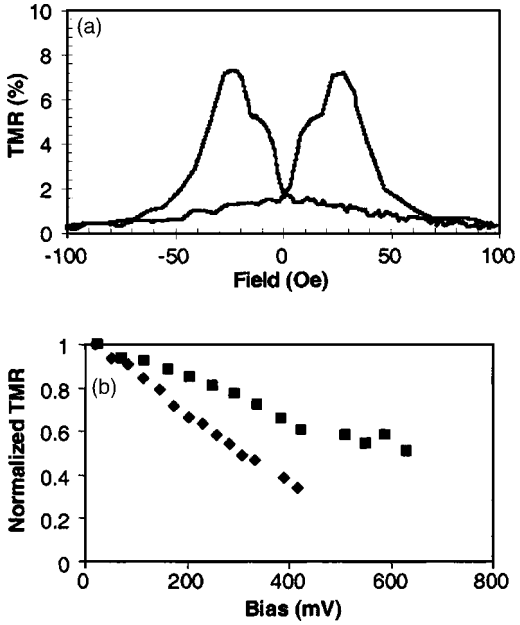

FIG. 3. (a) The TMR characteristic measured between the $(Ni_{81}Fe_{19})_e$ and Co_c electrodes of a DBMTJ, grown on quartz, with the Co_b electrode floating is shown for the $\theta=50°$ azimuth. (b) The bias dependence of the normalized TMR measured between the $(Ni_{81}Fe_{19})_e-Co_b$ (♦) and $(Ni_{81}Fe_{19})_e-Co_c$ (■) electrodes is shown.

formed to detect the transfer of hot electrons across the base layer as shown schematically in Fig. 1(b) and as described previously in Sec. II. For comparison we first present the results obtained from a sample grown on Si/SiO_2 in Fig. 5. The I_c-V_{eb} curve in Fig. 5(b) shows a region of negative slope at low bias. However, a current was also detected when R_3 was instead connected between the base and the collector lead of the other DBMTJ upon the substrate. This suggests that substrate leakage allows electrons to travel directly from the emitter to the collector before being returned to the base through the shorting resistor. The collector magnetocurrent was measured by sweeping the magnetic field while holding the value of V_{eb} fixed. The magnetocurrent was found to be largest near the values of V_{eb} at which the collector current changed sign. This behavior was not reproduced in samples deposited on quartz substrates, as may be seen from Fig. 6. The magnitude of I_c is similar to that observed for the sample on the Si/SiO_2 substrate, but now the I_c-V_{eb} characteristic has a positive slope over the full bias range. The magnetocurrent has a maximum value of 60% at low bias, and then decreases monotonically with increasing V_{eb}, reaching a value of just a few percent when $-V_{eb}=1000$ mV.

The form of the magnetocurrent curves obtained from many samples grown on both Si/SiO_2 and quartz substrates generally appeared as a weighted superposition of the individual barrier TMR curves. Figure 7 shows the magnetocurrent curves obtained from a second sample grown on quartz substrates for three different values of V_{eb}. The magnetocurrent curve is reminiscent of the emitter-base TMR at low bias, but becomes more similar to a base-collector TMR characteristic as V_{eb} becomes more negative.

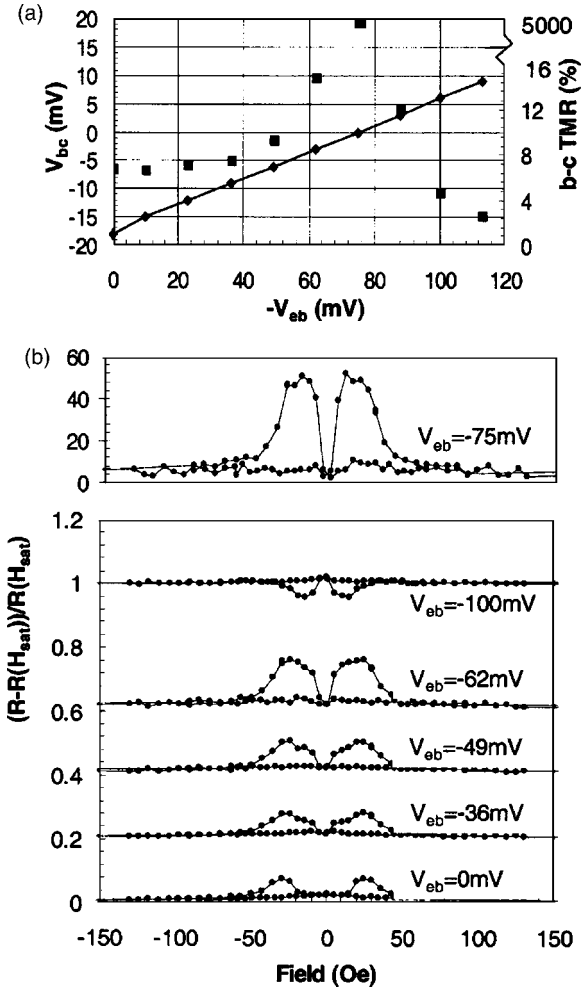

FIG. 4. (a) The dependence of the Co_b-Co_c junction TMR and the measured value of V_{bc} upon V_{eb} is shown for a DBMTJ grown upon a quartz substrate. A bias of 18 mV was applied to the $b-c$ circuit. (b) The shape of the Co_b-Co_c TMR characteristic at $\theta=50°$ is shown for different values of V_{eb}. The lower 6 curves have been offset for clarity.

IV. DISCUSSION

The characterization of the individual barriers within the sample grown on quartz demonstrates that junctions with a diameter as large as 0.5 mm may be successfully deposited

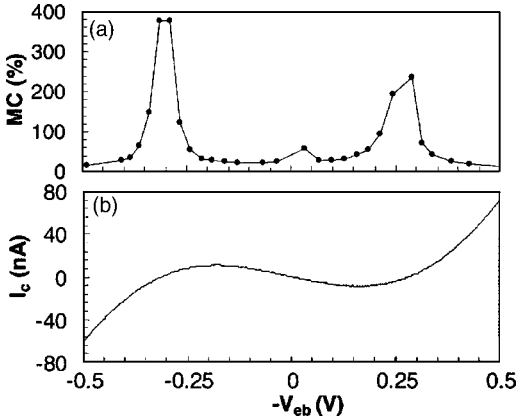

FIG. 5. (a) The bias dependence of the magnetocurrent obtained from a DBMTJ grown on a Si/SiO_2 substrate is shown (b) The corresponding I_c-V_{eb} characteristic is shown.

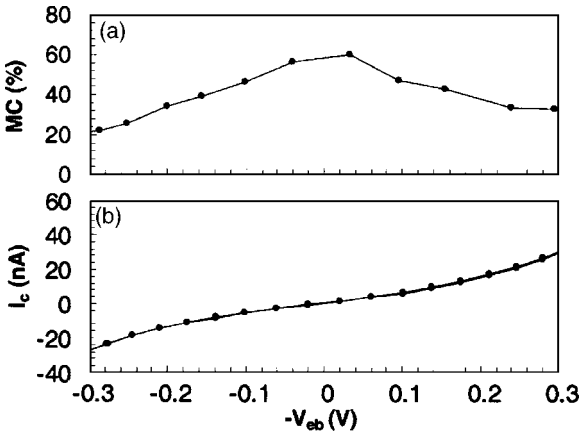

FIG. 6. (a) The bias dependence of the magnetocurrent obtained from a DBMTJ grown on a quartz substrate is shown (b) The corresponding I_c-V_{cb} characteristic is shown.

by means of the shadow mask method. The barrier resistances of approximately 1 kΩ are about two orders of magnitude greater than the sheet resistance of the electrodes and so current crowding effects are not expected to influence the TMR measurements made upon the individual barriers.[18–20] Furthermore we see that the fabrication method allows room-temperature TMR values of about 10% to be obtained for both barriers within a DBMTJ with a contact to the middle base electrode.

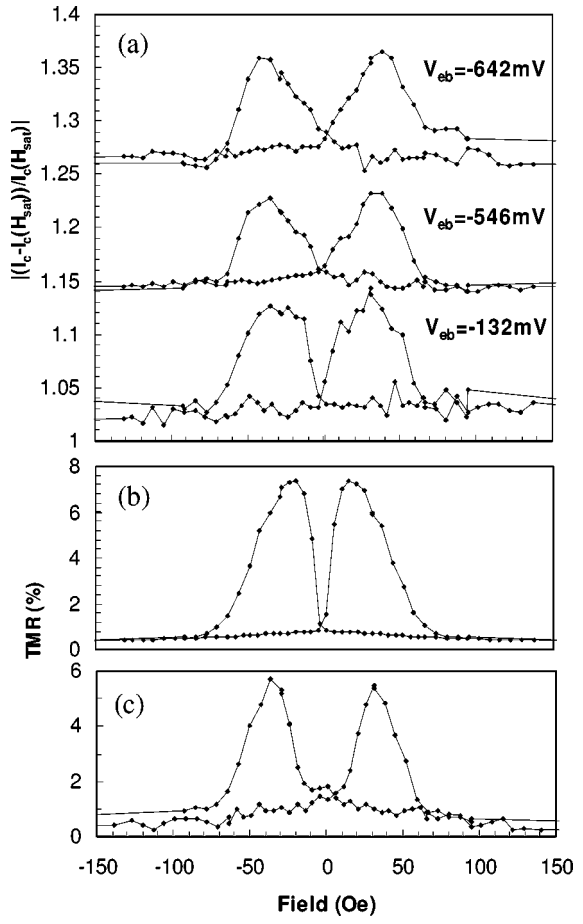

FIG. 7. (a) Magnetocurrent characteristics obtained from a second DBMTJ grown on a quartz substrate at θ=110° with different values of V_{eb} are shown. (b) The $(Ni_{81}Fe_{19})_e-Co_b$ TMR measured at θ=110° and 20 mV bias. (c) The Co_b-Co_c TMR measured at θ=110° and 20 mV bias.

The measurements made between the emitter and collector, with the base floating, do not show any significant enhancement of the TMR relative to that of the individual barriers. The double Julliere model[11] predicts a large TMR in the low bias regime due to coherent transport across the base layer. The switching of the electrode magnetizations in our sample is rather different and more complicated than that assumed in the model. However, the absence of any enhancement of the TMR suggests that the transport between the emitter and collector is incoherent in the present case. The observed bias dependence of the TMR also supports this conclusion. Since the two barriers have similar resistance, for incoherent transport, approximately half the applied voltage is dropped across each barrier, and so the double-barrier TMR decreases at half the rate of an individual barrier, as noted previously.[9]

A variation in the shape and height of the base-collector TMR curve was observed when a bias was applied simultaneously to the emitter-base junction, but this was accompanied by a variation in the measured V_{bc} value. Due to the finite resistance of the base electrode, simple application of Kirchoff's laws predicts that V_{bc} should exhibit a linear dependence upon V_1 and vanish at a point close to that observed in the experiment. However, since V_{bc} and I_c are both measured directly, the base-collector TMR is not expected to depend upon either the value of V_1 or the emitter-base TMR. Stein *et al.*[15] reported that the base-collector TMR was influenced by a current injected from the collector, although their experiments were performed somewhat differently with constant current sources in the emitter-base and base-collector circuits. They explained their observations in terms of diffusion of injected spin-polarized electrons across the base, leading to a modified polarization for tunneling at the base-collector interface. This mechanism would explain why the shape of the base-collector TMR curve increasingly resembles the emitter-base TMR curve as the emitter current is increased. Although the injected current density was two orders of magnitude smaller in our experiment compared to that of Stein *et al.* we note that the spin-diffusion length is not well known. Alternatively, due to the finite sheet resistance of the electrodes, we must also consider the small potential difference generated within the electrodes across the area of the base-collector barrier. When V_1 is adjusted so that the measured value of V_{bc} vanishes, there will be regions of small positive and negative bias within the area of the base-collector barrier due to the different geometries of the emitter-base and base-collector circuits. Interpretation of the TMR is then more complicated and it is known that nonuniform bias may lead to anomalously large measured TMR values.[8–20]

Samples grown upon Si/SiO_2 substrates showed a nonmonotonic I_c-V_{eb} characteristic. This can be understood if I_c has contributions of opposite sign due to substrate leakage and the base-collector tunnel current. We suggest that the substrate leakage and the base-collector tunnel current dominate at low and high bias, respectively. The large magnetocurrent observed in Si/SiO_2 samples is therefore an artifact resulting from the partial cancellation of the two currents. Specifically, the difference in the collector current measured

in the parallel and antiparallel configurations is normalized to a reduced value, exaggerating the apparent magnetocurrent value.

Although large magnetocurrent values have been observed within our DBMTJs, the I_c-V_{eb} characteristics are not of the form expected for ballistic transport of hot electrons across the base layer of the structure. Firstly, the measured I_c-V_{eb} curves do not have the expected asymmetry, and secondly the magnitude of I_c is too large. The probability that an injected electron that has crossed the base layer without being scattered will then tunnel into the collector is of the order of $\exp[-2\sqrt{2m(E-V)}d/\hbar]$ where m is the electron mass, d is the barrier thickness, and E and V are the electron energy and barrier height relative to the Fermi level in the base. This defines the maximum possible transfer ratio of collector current to emitter current. For the base-collector barrier discussed previously ($d=19$ Å, $\phi=1.94$ eV), an excess energy E of 0.3 eV leads to a maximum possible transfer ratio of order 10^{-11}. The hot-electron transfer ratio will be further reduced by inelastic scattering in the base layer, and it is likely that the Simmons fit provides a lower limit on the barrier height for ballistic electron transport when the barrier height is spatially nonuniform. We therefore conclude that the hot-electron current is too small to explain the transfer ratio of 10^{-4} observed in Fig. 5(b).

The resistance of each tunnel barrier in the present samples is sufficiently large that geometrical artifacts are not expected to modify the TMR measured across a single barrier in a two-terminal measurement.[18–20] However, this mechanism must be reexamined for the case of three-terminal measurements where the collector current is expected to be much smaller than the injected base current. Due to the finite sheet resistance of the base electrode, a current in the emitter-base circuit leads to a small voltage drop across the area of the base-collector junction. This implies that a small current can flow between the two edges of the base electrode by passing through the tunnel barrier and back through the resistor connected between the base and collector leads. The magnitude of the collector current may be estimated from

$$I_c \sim G\frac{R_{b,\square}I_b}{R_{Jn,bc}}, \tag{1}$$

in which G is a geometry-dependent factor with value of the order of 0.1. Since $R_{b,\square}/R_{bc}\approx 10^{-2}$ and $I_b\approx I_e$, we would expect to observe a transport ratio $I_c/I_e\approx 10^{-3}$, that is of similar magnitude to the measured value. Also the geometrical contribution to the current is present for both positive and reverse bias of the emitter-base barrier, as we observe, and is sensitive to the orientation of the magnetic electrodes. Ignoring the AMR of the base electrode, the change in the collector current due to the applied magnetic field is then given by

$$\frac{\Delta I_c}{I_c}\approx\frac{\Delta I_b}{I_b}-\frac{\Delta R_{bc}}{R_{bc}}=-(\mathrm{TMR})_{eb}-(\mathrm{TMR})_{bc}. \tag{2}$$

The collector magnetocurrent is therefore expected to appear as a weighted sum of the TMR characteristics of the individual tunnel barriers, where TMR_{eb} decreases rapidly with increasing V_{eb}, but TMR_{bc} is constant and corresponds to the value measured at $V_{bc}\approx 0$. The shape of the magnetocurrent curves should therefore change from being reminiscent of the emitter-base TMR values at low bias to being similar to the base-collector TMR at large bias values. This trend was observed in most of the samples studied, but it is surprising that the observed magnetocurrent values exceed the sum of the two TMR values. While this may again be related to the nonuniformity of the bias voltage within the area of the base-collector junction, we cannot exclude the possibility that electrons inelastically scattered within the base retain some memory of their initial spin state and so modify the effective spin polarization at the base-collector barrier.

V. CONCLUSIONS

In summary, three-terminal DBMTJs have been fabricated on Si/SiO_2 and quartz substrates for which the individual tunnel barriers exhibit significant room-temperature TMR and nonlinear $I-V$ characteristics. The TMR of the base-collector barrier was found to be strongly modified by injection of current through the emitter-base barrier. Spin diffusion across the base and a nonuniform voltage bias may be responsible although it is difficult to separate their relative effects. Measurements made on samples grown on Si substrates with the base and collector connected directly together showed large magnetocurrent values and a nonmonotonic I_c-V_{eb} characteristic. This behavior may be explained by the partial cancellation of contributions to the collector current due to substrate leakage and a geometrical artifact. Samples grown on quartz showed no evidence of substrate leakage and the observed magnetocurrent effects may be explained in terms of a geometrical artifact rather than hot-electron transport. In order to increase the relative contribution of the hot-electron transport a base-collector barrier with a lower barrier height, such as tantalum oxide[25] may be needed.

ACKNOWLEDGMENTS

We gratefully acknowledge the financial support of the Engineering and Physical Sciences Research Council (EPSRC) Seagate Technology, and the New Energy and Industrial Technology Development Organization (NEDO).

[1] J. S. Moodera and G. Mathon, J. Magn. Magn. Mater. **200**, 248 (1999).
[2] M. Julliere, Phys. Lett. **54**, 225 (1975).
[3] J. Slonczewski, Phys. Rev. B **27**, 6995 (1989).
[4] S. S. P. Parkin, Z. G. Li, and D. J. Smith, Appl. Phys. Lett. **58**, 2710 (1991).
[5] D. J. Monsma, J. C. Lodder, Th. J. A. Popma, and B. Dieny, Phys. Rev. Lett. **74**, 5260 (1995).
[6] R. Sato and K. Mizushima, Appl. Phys. Lett. **79**, 1157 (2001).
[7] S. Van Dijken, X. Jiang, and S. S. P. Parkin, Appl. Phys. Lett. **80**, 3364 (2002).
[8] E. Yu. Tsymbal and D. G. Pettifor, Phys. Rev. B **54**, 15314 (1996).
[9] S. Collis, G. Gieres, L. Bar, and J. Wecker, Appl. Phys. Lett. **83**, 948 (2003).
[10] F. Montaigne, J. Nasser, A. Vaures, F. Nguyen Van Dau, F. Petroff, A. Schuhl, and A. Fert, Appl. Phys. Lett. **73**, 2829 (1998).
[11] H. Lee *et al.*, J. Magn. Magn. Mater. **240**, 137 (2002).
[12] X. F. Han, S. F. Zhao, F. F. Li, T. Daibou, H. Kubota, Y. Ando, and T. Miyazaki, J. Magn. Magn. Mater. **282**, 225 (2004).
[13] M. Hehn, F. Montaigne, and A. Schuhl, Phys. Rev. B **66**, 144411 (2002).

[14]M. Heiblum and M. V. Fischetti, IBM J. Res. Dev. **34**, 530 (1990).
[15]S. Stein, R. Schmitz, and H. Kohlstedt, Solid State Commun. **117**, 599 (2001).
[16]D. Lacour *et al.*, Europhys. Lett. **60**, 896 (2002).
[17]N. D. Hughes and R. J. Hicken, J. Phys. D **35**, 3153 (2002).
[18]J. S. Moodera, L. R. Kinder, J. Nowak, P. Leclair, and R. Meservey, Appl. Phys. Lett. **69**, 708 (1996).
[19]J. S. Moodera, L. R. Kinder, and J. Nowak, J. Appl. Phys. **81**, 5522 (1997).
[20]K. Matsuda, N. Watari, A. Kamijo, and H. Tsuge, Appl. Phys. Lett. **77**, 3062 (2000).
[21]J. G. Simmons, J. Appl. Phys. **35**, 2655 (1964).
[22]E. Hartman, J. Appl. Phys. **35**, 3283 (1964).
[23]J. M. F. Gillies, A. E. T. Kuiper, and J. B. A. Van Zon, Appl. Phys. Lett. **78**, 3496 (2001).
[24]J. D. R. Buchanan, T. P. Hase, B. K. Tanner, N. D. Hughes, and R. J. Hicken, Appl. Phys. Lett. **81**, 751 (2002).
[25]P. Rottlander, M. Hehn, and A. Schuhl, Phys. Rev. B **65**, 054422 (2002).